Synthesis and characterisation of methylammonium borohydride

Kathryn R. Graham, Mark E. Bowden, and Tim Kemmitt .

Supporting Information

Table S1. Powder XRD peaks of $[CH_3NH_3]^+[BH_4]^-$.

hkl	d_{calc}	d_{obs}	I_{obs}
0 0 1	8.908	8.932	10
0 0 2	4.454	4.459	86
0 1 1	4.326	4.330	45
1 1 0	3.499	3.502	100
0 1 2	3.311	3.312	18
0 0 3	2.969	2.971	7
1 1 2	2.752	2.754	22
0 2 0	2.474	2.476	16
1 1 3	2.264	2.264	3
0 0 4	2.227	2.228	2
0 2 2	2.163	2.163	6
2 1 1	2.148	2.149	5
0 1 4	2.031	2.032	0.8
2 1 2	1.9819	1.9825	0.3
0 2 3	1.9009	1.9031	0.8
1 1 4	1.8788	1.8789	0.6
0 0 5	1.7817	1.7812	1.4
2 2 0	1.7496	1.7504	1.5
0 1 5	1.6763	1.6765	0.7
2 2 2	1.6285	1.6274	1.0
1 1 5	1.5877	1.5890	1.3
3 1 0	1.5649	1.5655	0.7
3 1 2	1.4764	1.4769	0.8
0 2 5	1.4458	1.4469	0.7
0 1 6	1.4221	1.4234	0.6

Table S2. Powder XRD peaks of $[BH_2(CH_3NH_2)_2]^+BH_4^-$. Indexed on orthorhombic unit cell a = 6.3173(4), b = 8.3777(5), c = 14.6016(10) Å. Possible space group $P2_12_12_1$.

h k l	d_{calc}	d_{obs}	I_{obs}
0 0 2	7.301	7.301	10
0 1 1	7.267		
1 0 1	5.798	5.812	72
0 1 2	5.504	5.515	42
1 1 0	5.044	5.053	32
1 1 1	4.768	4.776	94
0 1 3	4.209	4.198	80
0 2 0	4.189		
1 1 2	4.150	4.156	100
0 2 1	4.026	4.032	11
1 0 3	3.856	3.860	15
0 0 4	3.650	3.647	7
0 2 2	3.633		
1 1 3	3.502	3.503	30
1 2 1	3.395	3.399	41
0 1 4	3.347	3.350	21
0 2 3	3.175	3.167	31
1 0 4	3.161		
2 0 1	3.087	3.089	12
1 1 4	2.957	2.960	3
2 0 2	2.899	2.900	4
2 1 1	2.897		
1 2 3	2.837	2.839	5
2 1 2	2.740	2.742	5
1 0 5	2.651	2.653	1.4
0 3 2	2.608	2.608	1.5
1 3 0	2.554	2.556	1.6
2 2 0	2.522	2.523	20
1 3 1	2.516		
0 3 3	2.422	2.422	4
0 2 5	2.396	2.399	6
0 1 6	2.337	2.338	5
2 1 4	2.297	2.298	3
1 0 6	2.271	2.265	6
1 3 3	2.262		
1 2 5	2.240	2.242	4
0 3 4	2.218	2.218	3
1 1 6	2.192	2.193	2
2 3 0	2.092	2.091	7
3 0 1	2.084	2.080	6
2 1 5	2.077		
0 1 7	2.024	2.024	5
3 0 2	2.023		
0 4 2	2.013	2.014	4
1 4 1	1.9698	1.9688	3
3 1 2	1.9668		
0 4 3	1.9239	1.9248	1.7
3 2 0	1.8814	1.8825	1.5
3 2 1	1.8660	1.8662	1.6
3 0 4	1.8240	1.8226	2
3 2 2	1.8219		
2 3 4	1.8152	1.8164	2
1 3 6	1.7619	1.7598	2
1 4 4	1.7459	1.7467	2
3 2 4	1.6724	1.6724	1.7
3 3 3	1.5892	1.5885	1.2
0 4 7	1.4780	1.4786	1.8

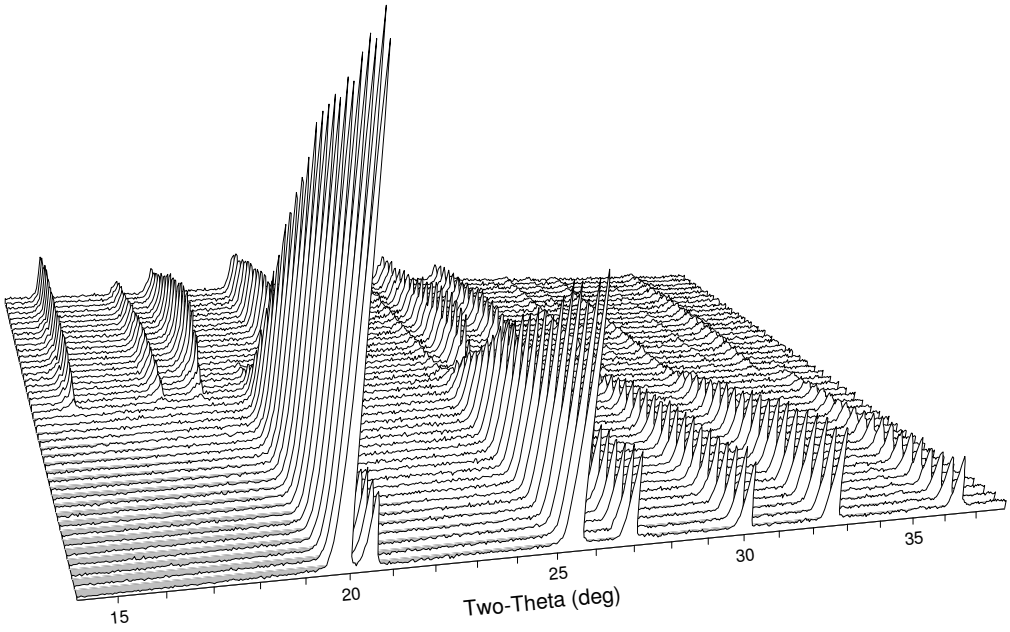

Figure S1. Transformation of $[CH_3NH_3]^+[BH_4]^-$ (front) to $[BH_2(CH_3NH_2)_2]^+BH_4^-$ (back) monitored by *in-situ* X-ray powder diffraction (Cu Kα radiation). No intermediate phases are observed.

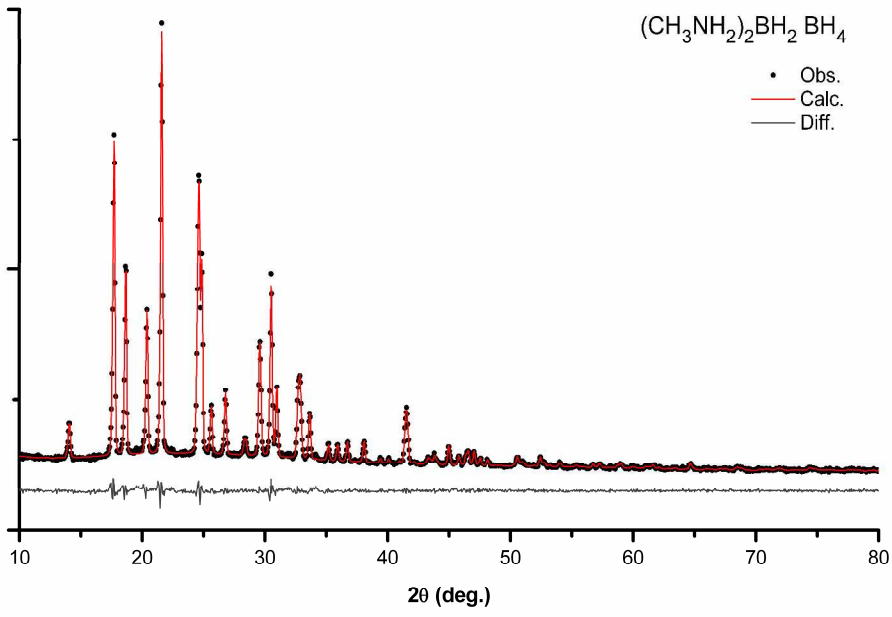

Figure S2. Calculated X-ray powder pattern for orthorhombic unit cell (*a* = 6.3173, *b* = 8.3777, *c* = 14.6016 Å) fitted to observed trace for $[BH_2(CH_3NH_2)_2]^+BH_4^-$.

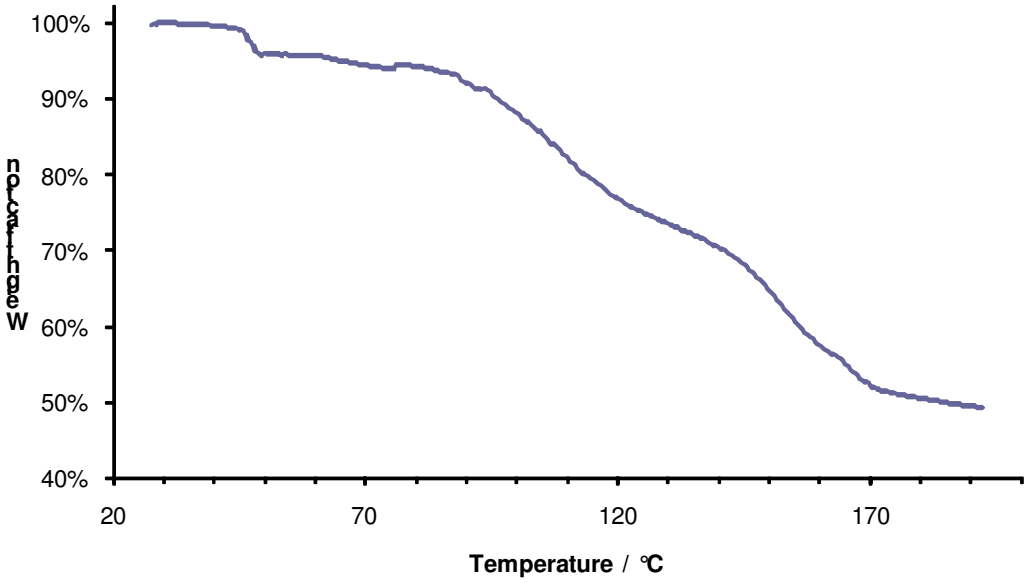

Figure S3. TGA trace of the thermal decomposition of $CH_3NH_3BH_4$ (Netzsch STA 449, 1°/min, 25 mL/min Ar). The weight loss above 70 °C is too large to be assigned to hydrogen loss and indicated volatilization of compounds such as $CH_3NH_2BH_3$ and $(CH_3NHBH_2)_3$

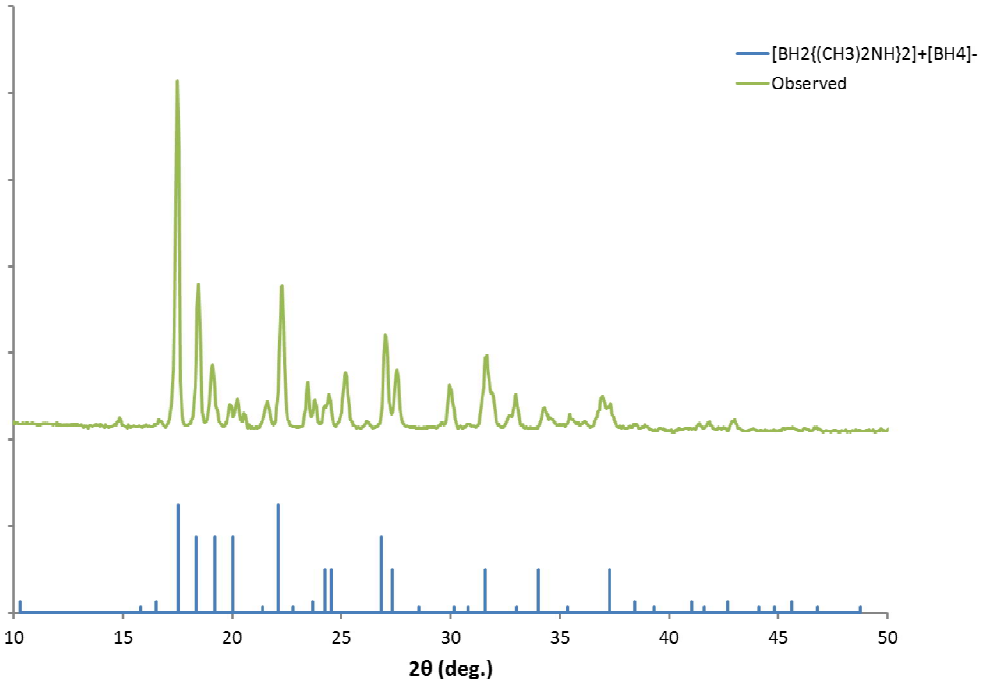

Figure S4. X-ray powder pattern of decomposition product from $(CH_3)_2NH_2BH_4$ compared with the literature pattern of $[BH_2\{(CH_3)_2NH\}_2]^+[BH_4]^-$.